第 31 卷第 5 期
2015 年 5 月

无 机 化 学 学 报
CHINESE JOURNAL OF INORGANIC CHEMISTRY

Vol.31 No.5
880-887

水热法制备树叶状 $LiFePO_4$/C 复合正极材料

云 强[1,2] 周 园*,[1] 海春喜[1] 申 月[1] 李 翔[1,2] 张丽娟[1,2] 李 松[1,2] 丁秀萍[1]

([1]中国科学院青海盐湖研究所盐湖资源化学重点实验室,西宁 810008)

([2]中国科学院大学,北京 100049)

摘要: 采用柠檬酸辅助水热法合成了高分散性树叶状 $LiFePO_4$/C 复合正极材料。利用 X 射线衍射、傅里叶红外光谱、扫描电镜、高分辨率透射电镜和选区电子衍射分析了材料的形貌结构。结果表明,柠檬酸对树叶状 $LiFePO_4$/C 复合材料的形成具有促进作用。该材料的最大暴露晶面为(010)晶面,且分散性较好。与颗粒状 $LiFePO_4$/C 材料相比,该材料呈现出更高的放电比容量和更好的倍率性能,在 0.1C 和 5C 倍率下,放电比容量分别为 158 和 126 $mAh\cdot g^{-1}$,其原因是由于锂离子沿[010]方向的扩散距离缩短,从而使锂离子扩散系数显著增大。

关键词: 材料科学; 水热合成; 电化学; $LiFePO_4$/C; 树叶状; 柠檬酸

中图分类号: O646; TM912.9 **文献标识码**: A **文章编号**: 1001-4861(2015)05-0880-08

DOI: 10.11862/CJIC.2015.128

Hydrothermal Synthesis of Leaf-like $LiFePO_4$/C Cathode Composites

YUN Qiang[1,2] ZHOU Yuan*,[1] HAI Chun-Xi[1] SHEN Yue[1] LI Xiang[1,2]

ZHANG Li-Juan[1,2] LI Song[1,2] DING Xiu-Ping[1]

([1]*Key Laboratory of Salt Lake Resources Chemistry of Qinghai Province, Qinghai Institute of Salt Lakes, Chinese Academy of Sciences, Xining* 810008, *China*)

([2]*University of Chinese Academy of Sciences, Beijing* 100049, *China*)

Abstract: Highly-dispersed $LiFePO_4$/C composite with micro-leaf structure was synthesized by a facile citric acid-assisted hydrothermal method in this study. Crystal structure and morphology of samples were investigated by XRD, FTIR, SEM, HR-TEM and selected area electron diffraction (SAED). The characterization results indicate that citric acid accelerates the formation of leaf-like $LiFePO_4$/C composite. The as-prepared leaf-like $LiFePO_4$/C composite with an enlarged (010) plane has high dispersibility. By comparing the electrochemical properties of the $LiFePO_4$/C particles in our study, the $LiFePO_4$/C micro-leaves exhibit larger discharge capacity and better rate performance, which deliver a discharge capacity of 158 $mAh\cdot g^{-1}$ at 0.1C and 126 $mAh\cdot g^{-1}$ at 5C. The enhanced performance perhaps is attributed to the reduced Li-ion diffusion paths along the [010] direction and larger Li-ion diffusion coefficient.

Key words: materials science; hydrothermal synthesis; electrochemistry; $LiFePO_4$/C; micro-leaf; citric acid

Due to its high theoretical capacity (~170 $mAh\cdot g^{-1}$), high safety, good cycle stability and low cost, olivine lithium iron phosphate ($LiFePO_4$) cathode material makes large-scale applications of lithium ion

收稿日期:2015-01-27。收修改稿日期:2015-02-25。

国家高技术研究发展计划(863)(No.2013AA110100);国家重点基础研究发展计划(973)(No.2014CB660806);中国科学院“西部之光”人才培养计划(No.Y412041007);2014 年西宁市科技项目(No.2014-6-24)资助。

*通讯联系人。E-mail:zhouy@isl.ac.cn;会员登记号:S06N9495M1208。

batteries (LIBs), such as electric vehicles (EVs), hybrid electric vehicles (HEVs) and stationary energy storage for solar and wind electricity generation as well as smart grids[1-2]. However, large-scale applications of $LiFePO_4$ in different fields have been limited by both the low electronic conductivity from the separation of FeO_6 octahedra by PO_4^{3-} ions in the $LiFePO_4$ structure and the poor Li-ion mobility from the slightly distorted hexagonal close-packed oxygen array[2]. Therefore, considerable efforts have been made to improve its conductivity.

Generally, in order to improve the electronic conductivity of $LiFePO_4$, surface coating with a thin layer of conductive carbon[3], metal[4] or metal oxide[5], and conductive polymers[6], has been employed. Especially, *in-situ* surface modification by conductive elements is commonly regarded as one of the most successful methods to overcome the defects induced from the post-surface modification of insulator[7]. Meanwhile, the Li-ion mobility is accelerated by ion-doping at Li-site[8] or Fe-site[9], reducing the particle size[10], or tailoring the morphology and texture[11-13]. Benefiting from the smoothed diffusion channel of ions, tailoring the morphology and texture of materials is one of the most effective ways to improve the Li-ion mobility, thereby increasing its ionic conductivity. This conclusion also can be verified by the first principle calculation, which shows that Li-ions move preferentially via one dimensional channels oriented along the [010] direction in the olivine structure[14-15]. Therefore, preparation of $LiFePO_4$/C composite with a preferential growth along the (010) plane via an *in-situ* method could be a new strategy to improve the electrochemical performance of $LiFePO_4$ material.

Studies[10,16-18] suggest that plate-like $LiFePO_4$/C could be prepared by a solvothermal/hydrothermal method with ethylene glycol as solvent or sodium dodecyl benzene sulfonate as an anionic surfactant. Their results indicate that plate-like $LiFePO_4$/C with (010) plane not only reduces the Li-ion transport length, but also enlarges the (010) plane compared with $LiFePO_4$/C composites in other morphologies, thus resulting in fast Li-ion mobility. However, the agglomeration of the plate-like $LiFePO_4$/C prepared in these works is so serious that limits the improvement of their electrochemical performances.

Herein, we report the synthesis of highly-dispersed $LiFePO_4$/C micro-leaves oriented along the (010) plane by a facile citric acid-assisted hydrothermal method. By comparing with $LiFePO_4$/C composite prepared without citric acid, the electrochemical performance variation of $LiFePO_4$/C micro-leaves is also verified.

1 Experimental

1.1 Synthesis of $LiFePO_4$/C composites

$LiFePO_4$/C composites were synthesized through a combination of hydrothermal reaction and calcination process by employing Li_3PO_4, $FeSO_4 \cdot 7H_2O$, ascorbic acid and citric acid as reactants. All the chemicals (from Sinopharm Chemical Reagent Co. Ltd., China) were analytical grade and used without further purification. Firstly, $FeSO_4 \cdot 7H_2O$, ascorbic acid and Li_3PO_4 were added into 50 mL deionized water with the molar ratio of 1∶0.2∶1 and magnetically stirred for 20 min, where ascorbic acid acts as a reductant preventing the oxidation of divalent iron. Secondly, citric acid were added to the mixed suspension with the molar ratio of citric acid and $FeSO_4 \cdot 7H_2O$ as 1∶3, and magnetically stirred for 48 h. Thirdly, as-prepared mixtures were transferred into an 80 mL Teflon autoclave and followed by hydrothermal reaction at 180 ℃ for 10 h. After cooling naturally to room temperature, the products were thoroughly washed with deionized water and ethanol, and dried at 80 ℃ for 10 h. Finally, the precursors were calcined at 700 ℃ in argon for 10 h to get the target materials.

The blank sample was prepared by the same method without adding citric acid.

1.2 Stability comparison

0.15 g $LiFePO_4$/C prepared without/with citric acid in reaction systems were dispersed into 15 mL deionized water in ultrasonic bath for 20 min. After standing for 1 h, digital photos were taken.

1.3 Characterization

The composition and crystal structure of as-

prepared samples were identified by XRD on X′pert PRO X-ray diffractometer (Panalytical B. V. Company, Holland) using Cu $K\alpha$ radiation sources (λ=0.154 18 nm) in the range of 10°~70° (X′celerator new high-performance detector, tube voltage: 40 kV, tube current: 40 mA). The carbon contents of the samples were detected by the elemental analyzer (Vario EL cube, Elementar Company, Germany). FTIR spectra were collected at room temperature on a Thermo-Nicolet Nexus FTIR spectrometer (USA) equipped a KBr crystal in the absorbance mode range from 400 to 4 000 cm^{-1} with a resolution of 2 cm^{-1}. The morphology was observed by scanning electron microscopy (SEM, JEOL, JSM-5610LV/INCA) at 20 kV and field-emission transmission electron microscope (FETEM, TECNAI G^2 TF20) at 200 kV.

1.4 Electrochemical measurements

To prepare the $LiFePO_4$ cathode electrodes, a uniformly *N*-methyl-2-pyrrolidone (NMP) slurry, containing active material, super-P and polyvinylidene fluoride (PVDF) with the weight ratio of 80∶10∶10, was coated on aluminum foil and dried at 60 ℃ in air for 2 h and followed by drying at 120 ℃ in vacuum for 12 h. The electrolyte was 1 mol·L^{-1} $LiPF_6$ in mixed solvent of ethylene carbonate (EC), dimethyl carbonate (DMC) and diethyl carbonate (DEC) with 1∶1∶1 in volume ratio. Lithium (Shenzhen Kejinstar Technology Co. Ltd., China) and Celgard 2400 (America) were used as anode and separator, separately.

The electrochemical properties of the cathode materials were characterized by assembling CR2032 coin-type cell in a glove box filled with high-purity argon gas. Galvanostatic charge-discharge cycling tests of the assembled cells were carried out on electrochemical test instrument (CT2001A, Wuhan Land Electronic Co. Ltd., China) at various current rates in the voltage range of 2.5~4.2 V (vs Li^+/Li). Cyclic voltammetry (CV) was performed at scan rate of 0.1 mV·s^{-1} in the voltage range of 2.5~4.2 V (vs Li^+/Li) on an electrochemical workstation (LK2005A, Tianjin Lanlike Electrochemical High-Tech Co. Ltd., China). The electrochemical impedance spectroscopies (EIS) were tested on an electrochemical workstation (AUTOLAB PGSTA T208, Metrohm China Ltd., China) with the excitation potential of 5 mV in frequency from 100 kHz to 0.1 Hz. All the electrochemical measurements were performed at room temperature.

2 Results and discussion

2.1 Structural and morphology analysis

Fig.1 presents the XRD patterns of $LiFePO_4$ obtained by hydrothermal synthesis without/with citric acid in reaction systems. All the diffraction peaks can be well indexed to an orthorhombic olivine space group, Pnma (PDF No.40-1499), which indicates that single-phase $LiFePO_4$ has been prepared without any observable impurity phases (such as Li_3PO_4 and $Li_3Fe_2(PO_4)_3$). The addition of citric acid does not change the crystal structure of $LiFePO_4$ by comparing the XRD patterns of Figs.1(a) and (b). In addition, the carbon contents of two samples are about 0.6wt% and 1.9 wt% separately, indicating that the carbon exists in two samples. The carbon in the blank sample comes from the breakdown of ascorbic acid, and the addition of citric acid increases the carbon content in the sample. However, no typical diffraction peaks of carbon are found in the XRD patterns, which may be attributed to the limited amount of phase [19] or the existence of amorphous carbon in our samples[20].

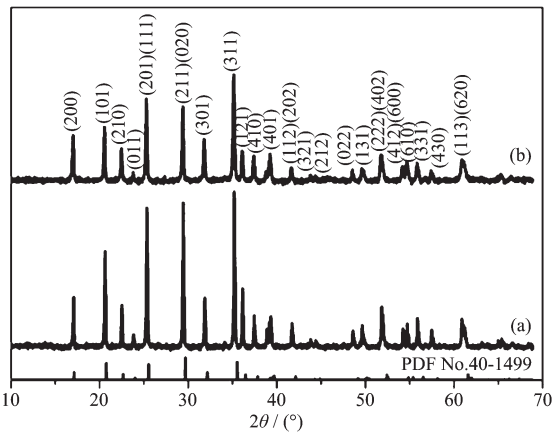

Fig.1 XRD patterns of $LiFePO_4$ (a) without citric acid and (b) with citric acid in reaction systems

Fig.2 displays the morphology of the $LiFePO_4$/C composites. As shown in Fig.2(a) and (b), without citric acid in reaction system, $LiFePO_4$/C composite is

agglomerated particles. While, adding the citric acid in reaction system results in the well-dispersed leaf-like $LiFePO_4$/C composites (Fig.2 (c) and (d)). The maximum size of the leaf-like $LiFePO_4$/C composite is 3.5 μm and the minimum one is 0.9 μm. The TEM image of $LiFePO_4$/C composite with citric acid in reaction system shown in Fig.3(a) further confirms that the observed $LiFePO_4$/C composite is micro-leaves. There are clear lattice fringes in HRTEM image of the $LiFePO_4$/C micro-leaves as shown in Fig.3(b), indicating that it is single-phase crystallinity for the $LiFePO_4$/C micro-leaves, which corresponds to the SAED image in Fig.3(c). Furthermore, the lattice fringe spacing in Fig.3(b) indicates that the largest exposed plane of the $LiFePO_4$/C micro-leaves is the (010) lattice plane.

Stability of as-prepared $LiFePO_4$/C composites in water is confirmed by Fig.4. The leaf-like $LiFePO_4$/C composite owns better stability. FTIR spectra shown in Fig.5 indicate that the relatively weak bands in the region of 440~650 cm^{-1} are corresponding to the bending O-P-O vibrations, and the P-O stretching vibrations are represented by the strong bands in the region of 1 180~920 cm^{-1} [21]. The stretching and bending vibrations of O-H are observed around 3 420 and 1 650 cm^{-1} separately, which implies the existence of -OH on the surface of evaluated specimens[22]. Maybe the intensified peak of -OH around 3 420 cm^{-1} attributes to the improved stability of the $LiFePO_4$/C micro-

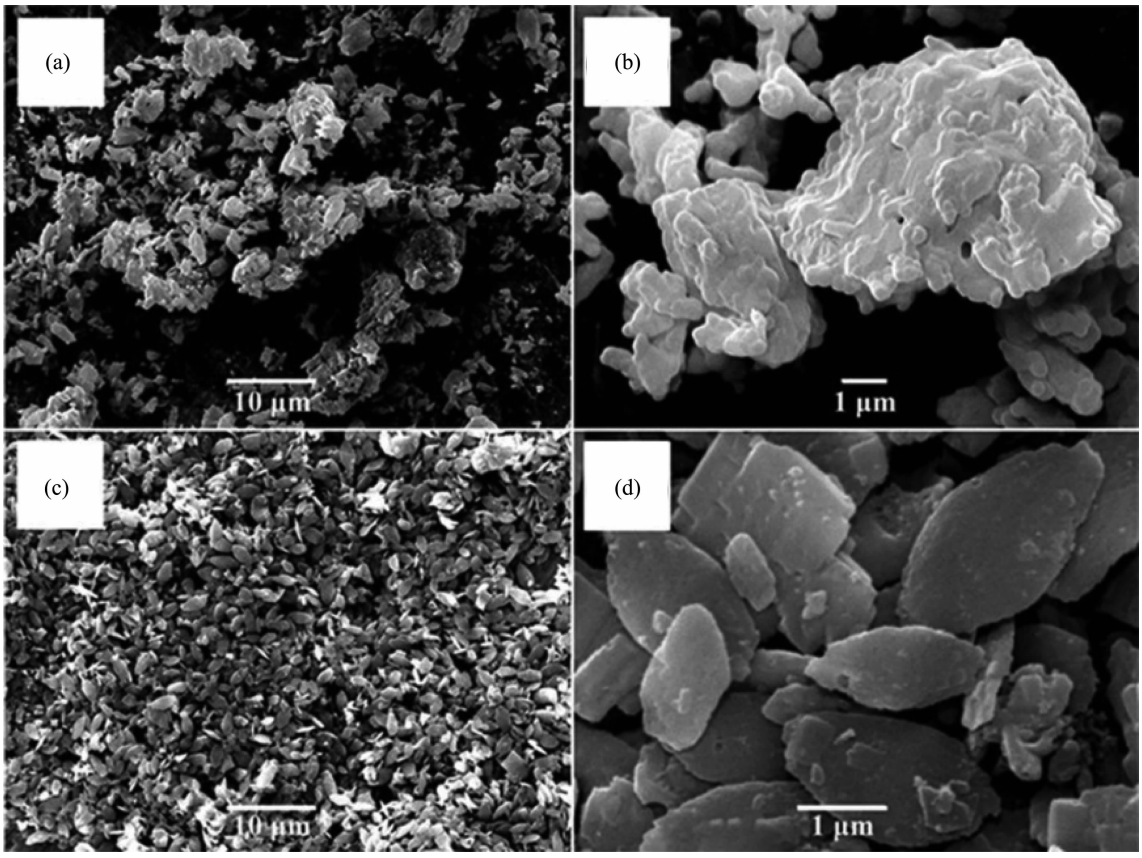

Fig.2　SEM images of the $LiFePO_4$/C composite prepared (a, b) with citric acid and (c, d) without citric acid

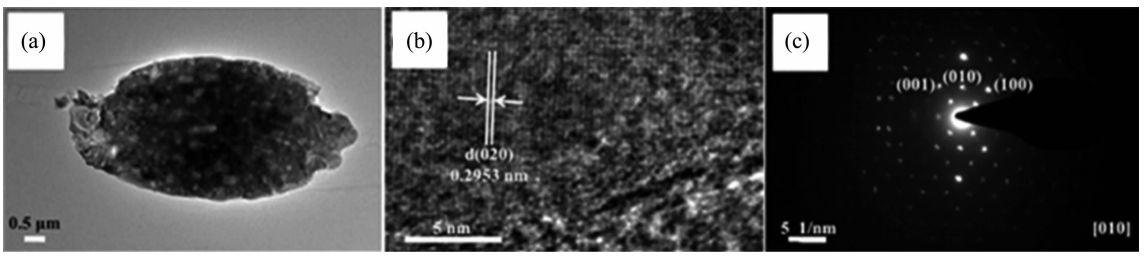

Fig.3　(a) TEM, (b) HRTEM and (c) SAED images of the $LiFePO_4$/C composite prepared with citric acid

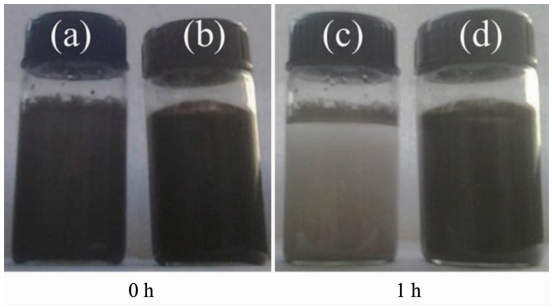

Fig.4 Dispersion state of (a, c) the $LiFePO_4$/C particles and (b, d) the $LiFePO_4$/C micro-leaves in water

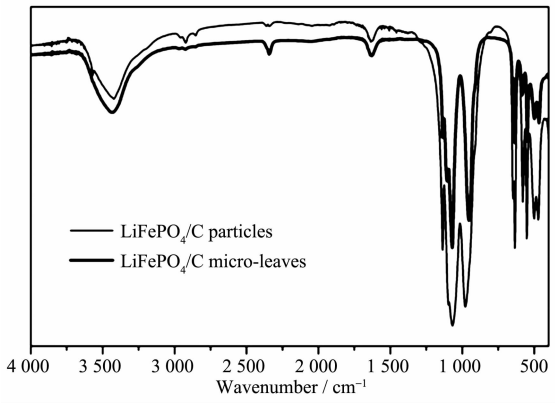

Fig.5 FTIR spectra of the $LiFePO_4$/C particles and the $LiFePO_4$/C micro-leaves

leaves in water.

We propose the formation mechanism of leaf-like $LiFePO_4$/C composite based on the above results. The first step is nucleation of $LiFePO_4$. As increasing the reaction temperature, Li_3PO_4 in the precursor begins to dissolve, and then the concentrations of $[Fe(H_2O)_n]^{2+}$, $[Li(H_2O)_n]^{+}$ and PO_4^{3-} build up[23]. The heterogeneous nucleation mechanism needs lower critical nucleation concentration than homogenous nucleation, so the nucleation of $LiFePO_4$ tends to be heterogeneous nucleation. The aquo-metal ions $[Fe(H_2O)_n]^{2+}$, $[Li(H_2O)_n]^{+}$ and PO_4^{3-} are transformed into the $LiFePO_4$ nuclei at the surface or edge of the Li_3PO_4 which is not completely dissolved in solution yet. The controlled dissolution of Li_3PO_4 perhaps attributes to the uniform nucleation of $LiFePO_4$.

The second step is the nuclei growth of $LiFePO_4$, which has a powerful influence on the final morphology of $LiFePO_4$ materials. The crystal growth is mainly controlled by the nuclei surface energy. Nuclei surfaces with high surface energy have greater ion adsorbing ability, so they have faster growth rate along the vertical direction of nuclei surfaces. The surface energy of the (010) lattice plane for $LiFePO_4$ is smaller than that of other lattice planes[15]. In addition, in water, $LiFePO_4$ is hydroxylated, forming -FeOH on the surface of $LiFePO_4$, which is also confirmed by FTIR spectra in Fig.5. These hydroxyl groups can form hydrogen bond with the carboxyl groups of citric acid[16]. Hence, as shown in Fig.6, citric acid molecules could be more easily absorbed on the (010) lattice plane of $LiFePO_4$ crystal nucleis via hydrogen banding force, and further decrease the surface energy of (010) lattice plane[17], then causing the preferential growth of the $LiFePO_4$ crystals along their parallel direction, leading to the highly-dispersed $LiFePO_4$/C micro-leaves.

2.2 Electrochemical properties

Fig.7 shows the charge-discharge curves of the $LiFePO_4$/C particles and micro-leaves at various current rates from 0.1C to 5C in the voltage range of 2.5 ~4.2 V vs Li^+/Li. The discharge curves of two composites at 0.1C exhibit a perfect plateau voltage of 3.4 V vs Li^+/Li, indicating a typical two-phase reaction between $FePO_4$ and $LiFePO_4$. Comparing the charge-discharge curves of two samples, the $LiFePO_4$/C particles has shorter charge-discharge plateau at all discharge rates. As shown in Fig.7(a), the $LiFePO_4$/C particle delivers a discharge capacity of 125 $mAh \cdot g^{-1}$ with a voltage plateau near 3.4 V vs Li^+/Li at a low current rate of 0.1C. When the current rate is increased to 1C, the $LiFePO_4$/C particles deliver a

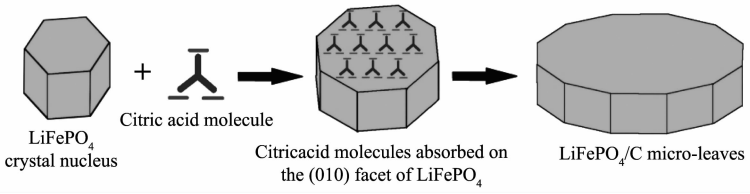

Fig.6 Schematic illustration for the formation process of $LiFePO_4$/C micro-leaves

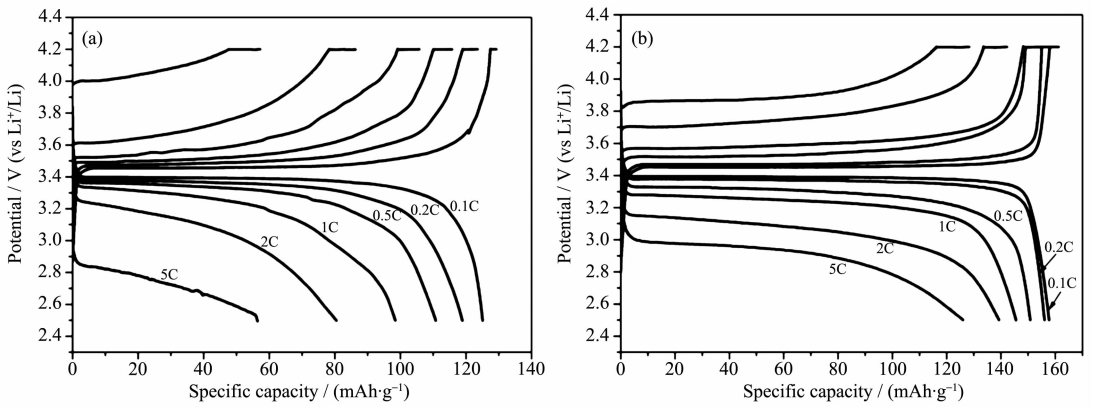

Fig.7　Charge-discharge curves of (a) the $LiFePO_4$/C particles and (b) the $LiFePO_4$/C micro-leaves in the potential range of 2.5~4.2 V at various current rates

discharge capacity of 99 mAh·g^{-1}. When the current rate is further increased to 5C, the discharge capacity significantly decreases to 56 mAh·g^{-1}, and the voltage plateau shrinks greatly. However, the result shown in Fig.7(b) suggests that the highly-dispersed $LiFePO_4$/C micro-leaves exhibit excellent rate performance. Discharge capacity of the $LiFePO_4$/C micro-leaves can reach 158 mAh·g^{-1} at 0.1C. Even when the current rate further increases to 5C, the discharge capacity can still reach 126 mAh·g^{-1} and the voltage plateau remains distinct. Comparing with that of the plate-like $LiFePO_4$/C in related literatures [10,17-18], the rate performance of the $LiFePO_4$/C micro-leaves prepared in our study also has been improved. More, the capacity retention is 80% compared with the capacity at 0.1C. The results from Fig.7 demonstrate that the highly-dispersed $LiFePO_4$/C micro-leaves have good electron conductivity, low polarization, as well as good rate performance.

Fig.8 exhibits a comparison of the rate and cycling performances of the $LiFePO_4$/C particles and micro-leaves. The discharge capacities of two samples remain stable and decrease with an increased current rate. Comparing with that of the $LiFePO_4$/C particles, the discharge capacity of the highly-dispersed $LiFePO_4$/C micro-leaves is greatly enhanced at current rates from 0.1C to 5C, especially at higher current rates. When the current rate is decreased from 5C to 0.2C and 0.5C, the capacities retentions of the $LiFePO_4$ micro-leaves are still 98% and 97% separately. The good cycling performance may be mainly ascribed to the good electrochemical reversibility and structural stability of phosphor-olivine $LiFePO_4$[2]. Perhaps there are two reasons for the enhanced rate capability of leaf-like $LiFePO_4$/C composite. Firstly, the highly-dispersed $LiFePO_4$/C micro-leaves with (010) plane synthesized by citric acid-assisted hydrothermal method can reduce the distance of Li-ion diffusion along the [010] direction, which enhances the Li-ion diffusion rate[12,17]. Secondly, the increase of surface area of (010) plane is active for Li-ion intercalation/extraction[24].

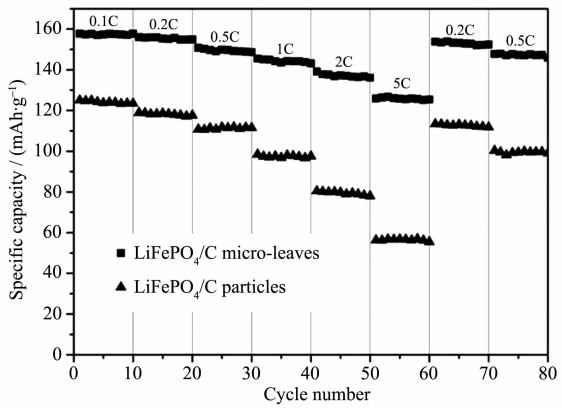

Fig.8　Rate and cycling performances of the $LiFePO_4$/C particles and the $LiFePO_4$/C micro-leaves

Fig.9 shows the CV profiles of the $LiFePO_4$/C particles and micro-leaves at a scan rate of 0.1 mV·s^{-1} from 2.5 V to 4.2 V. The CV curves show a pair of anodic and cathodic peaks, which correspond to the two-phase intercalation/extraction of Li-ions involving an Fe^{2+}/Fe^{3+} redox couple. The higher peak of the $LiFePO_4$/C micro-leaves indicates that they possess a larger high-rate capability than the $LiFePO_4$/C particles.

The separation potential of $LiFePO_4$/C particles is 0.4 V, whereas that of the $LiFePO_4$/C micro-leaves is 0.3 V. The more symmetric and spiculate peak profile for the $LiFePO_4$/C micro-leaves suggests that the reversibility of the electrochemical reaction during Li-ion insertion and extraction is greatly enhanced.

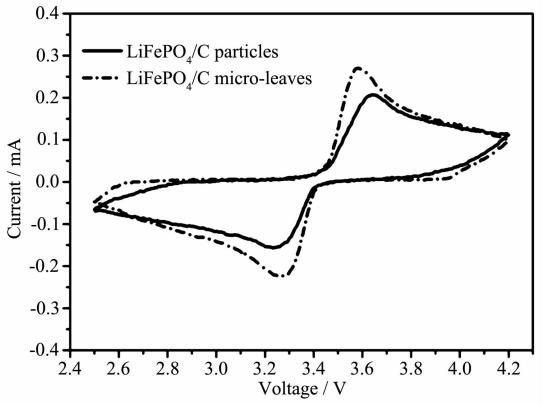

Fig.9 CV profiles of the $LiFePO_4$/C particles and the $LiFePO_4$/C micro-leaves at a scan rate of 0.1 $mV \cdot s^{-1}$ in the potential range of 2.5~4.2 V

The EIS spectra of the $LiFePO_4$/C particles and micro-leaves are shown in Fig.10(a). Both EIS profiles exhibit a semicircle in high frequency region and a straight line in low frequency region. The intercept impedance in the high frequency region of the Z' real axis corresponds to the ohmic resistance (R_e) of the electrolyte, separator, and electrode. The semicircle in the middle frequency region indicates the charge transfer resistance (R_{ct}). The straight line in low frequency region is attributed to the Warburg impedance (Z_w), which is related to the Li-ion diffusion in the $LiFePO_4$/C composites. The R_{ct} of the $LiFePO_4$/C micro-leaves is much smaller than that of the $LiFePO_4$/C particles, indicating that the reduced distance of Li-ion diffusion along the [010] direction enhances the electrochemical performance.

The Li-ion diffusion coefficients (D_{Li}) of the $LiFePO_4$/C particles and micro-leaves can be calculated according to the following equation:

$$D_{Li}=R^2T^2/(2A^2n^4F^4C^2\sigma^2) \quad (1)$$

where R is the gas contant, T is the absolute temperature, A is the electrode area, n is the number of electrons per molecule during oxidization, F is the Faraday constant, C is the concentration of Li-ion, and σ is the Warburg factor which has the relationship with Z':

$$Z'=R_e+R_{ct}+\sigma\omega^{-1/2} \quad (2)$$

Fig.10(b) shows the relationship between Z' and $\omega^{-1/2}$ at low frequency. According to the slopes of the lines, the Li-ion diffusion coefficients of the $LiFePO_4$/C particles and micro-leaves are calculated to be 3.5×10^{-15} and 1.1×10^{-14} $cm \cdot s^{-1}$ separately. The $LiFePO_4$/C micro-leaves with orientation along the (010) plane have larger Li-ion diffusion coefficient, which enhances their cycling and rate performance.

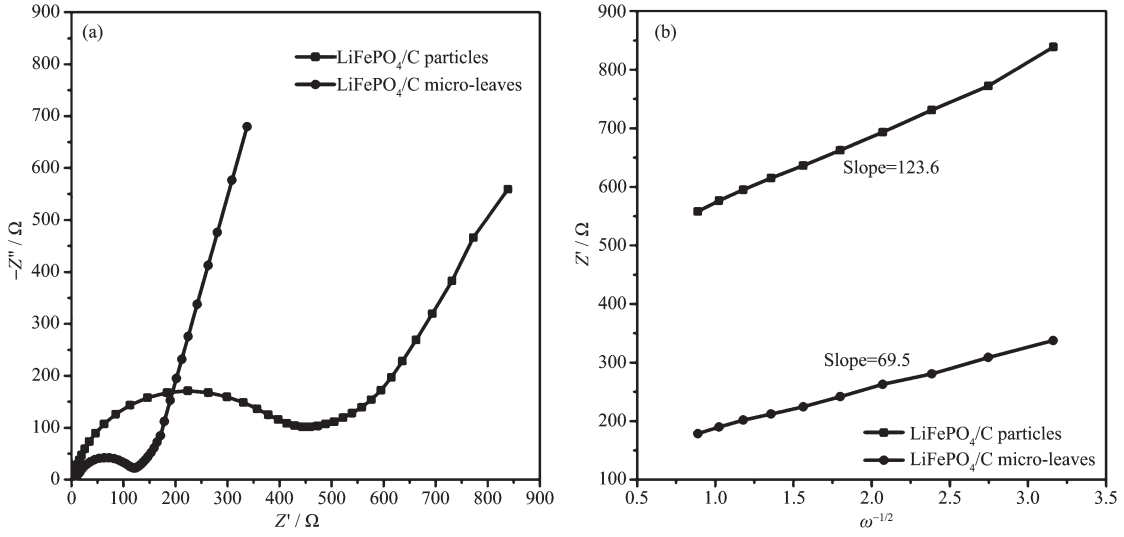

Fig.10 (a) EIS spectra of the $LiFePO_4$/C particles and the $LiFePO_4$/C micro-leaves; (b) Relationship between Z' and $\omega^{-1/2}$ at low frequency

3 Conclusions

In summary, highly-dispersed leaf-like $LiFePO_4$/C composite with orientation along the (010) plane has been prepared by a facile citric acid-assisted hydrothermal synthesis. As supported by characterization results, citric acid accelerates the formation of leaf-like $LiFePO_4$/C composite. Comparing with agglomerated particles, leaf-like $LiFePO_4$/C composite exhibits larger discharge capacity and better cycling and rate performance, which perhaps benefits from the reduced distance of Li-ion diffusion along the [010] direction and larger Li-ion diffusion coefficient.

References:

[1] Whittingham M S. *Chem. Rev.*, **2014**,**114**(23):11414-11443

[2] Padhi A K, Nanjundaswamy K S, Goodenough J B. *J. Electrochem. Soc.*, **1997**,**144**(4):1188-1194

[3] Xie G, Zhu H J, Liu X M, et al. *J. Alloys Compd.*, **2013**, **574**:155-160

[4] Lu Z G, Cheng H, Lo M F, et al. *Adv. Funct. Mater.*, **2007**, **17**(18):3885-3896

[5] Hu Y S, Guo Y G, Dominko R, et al. *Adv. Mater.*, **2007**,**19** (15):1963-1966

[6] Nguyen V H, Wang W L, Jin E M, et al. *J. Alloys Compd.*, **2013**,**569**:29-34

[7] Li H Q, Zhou H S. *Chem. Commun.*, **2012**,**48**(9):1201-1217

[8] Chung S Y, Chiang Y M. *Electrochem. Solid-State Lett.*, **2003**, **6**(12):A278-A281

[9] LUO Liang(罗亮), CAO Yan-Bing(曹雁冰), DU Ke(杜柯), et al. *Chinese J. Inorg. Chem.*(无机化学学报), **2014**,**30**(9): 2000-2005

[10]Yang H, Wu X L, Cao M H, et al. *J. Phys. Chem. C*, **2009**, **113**(8):3345-3351

[11]Pei B, Yao H X, Zhang W X, et al. *J. Power Sources*, **2012**, **220**:317-323

[12]Saravanan K, Balaya P, Reddy M V, et al. *Energy Environ. Sci.*, **2010**,**3**(4):457-463

[13]DONG Jing(董静), ZHONG Ben-He(钟本和), ZHONG Yan-Jun(钟艳君), et al. *Chinese J. Inorg. Chem.*(无机化学学报), **2013**,**29**(10):2257-2264

[14]Islam M S, Driscoll D J, Fisher C A, et al. *Chem. Mater.*, **2005**,**17**(20):5085-5092

[15]Fisher C A, Islam M S. *J. Mater. Chem.*, **2008**,**18**(11):1209-1215

[16]Mei R G, Song X R, Yang Y F, et al. *RSC Adv.*, **2014**,**4** (11):5746-5752

[17]Ma Z P, Shao G J, Wang X, et al. *Mater. Chem. Phys.*, **2014**, **143**(3):969-976

[18]HUANG Fu-Qin(黄富勤), TANG Xin-Chun(唐新春), XIAO Yuan-Hua(肖元化), et al. *Chinese J. Inorg. Chem.*(无机化学学报), **2014**,**30**(2):235-241

[19]Doeff M M, Wilcox J D, Kostecki R G, et al. *J. Power Sources*, **2006**,**163**(1):180-184

[20]Du J, Jiao L F, Wu Q, et al. *Electrochim. Acta*, **2013**,**98**: 288-293

[21]Muraliganth T, Murugan A V, Manthiram A. *J. Mater. Chem.*, **2008**,**18**(46):5661-5668

[22]Wu G, Zhou Y K, Shao Z P. *Appl. Surf. Sci.*, **2013**,**283**:999-1005

[23]Qin X, Wang X H, Xiang H M, et al. *J. Phys. Chem. C*, **2010**,**114**(39):16806-16812

[24]Kim D H, Kim J. *Electrochem. Solid-State Lett.*, **2006**,**9**(9): A439-A442